Ultraviolet Resonance Raman Examination of the Light-Induced Protein Structural Changes in Rhodopsin Activation†

Gerd G. Kochendoerfer, Shoji Kaminaka, and Richard A. Mathies*

Department of Chemistry, University of California, Berkeley, California 94720

Received June 26, 1997; Revised Manuscript Received August 21, 1997⊗

ABSTRACT: Ultraviolet resonance Raman (UVRR) spectra of rhodopsin and its metarhodopsin I and metarhodopsin II photointermediates have been obtained to examine the molecular mechanism of G-protein-coupled receptor activation. Spectra were acquired using a single-pass capillary flow technique in combination with a Littrow prism UV prefilter detection system. The UVRR difference spectra between rhodopsin and metarhodopsin I exhibit small differences assignable to tyrosine residues and no differences due to tryptophan. The UVRR difference spectra between rhodopsin and metarhodopsin II exhibit significant differences for vibrations of both tryptophan and tyrosine residues. Most importantly, there is an intensity decrease of the totally symmetric tryptophan modes at 759, 1008, and 1545 cm^{-1}, an intensity decrease of the tryptophan W7 band at 1357 cm^{-1}, and a frequency shift of the tryptophan W17 band from 885 to 892 cm^{-1}. These difference features are assigned to one or more tryptophan residues that reside in a hydrophobic, weakly hydrogen-bonding environment in rhodopsin and that are transferred to a less hydrophobic, non-hydrogen-bonding environment during rhodopsin activation. The available evidence suggests that Trp_{265} makes a dominant contribution to the tryptophan features in this difference spectrum. These results are interpreted with a model for rhodopsin activation in which retinal isomerization alters the interaction of Trp_{265} with the ionone ring of the retinal chromophore.

Rhodopsin is a seven α-helix intrinsic membrane protein and a member of the G-protein-coupled receptor family. The primary event in rhodopsin activation is an ultrafast 11-*cis* to *all-trans* isomerization of the 11-*cis*-retinal chromophore to form photorhodopsin (Kochendoerfer & Mathies, 1995; Schoenlein et al., 1991). This first photoproduct structurally relaxes via several thermal intermediates to form metarhodopsin II (meta II),[1] which is the active signaling state (Kliger & Lewis, 1995). The meta II state is characterized by an absorption maximum of 380 nm, the uptake of two protons, and the deprotonation of the retinal Schiff base. *In vivo* the meta II form of rhodopsin activates the G-protein transducin. This event triggers the signal amplification process and eventually results in the transduction of a nerve impulse (Hofmann et al., 1995). We are interested in understanding how chromophore isomerization is coupled to receptor activation.

Early studies showed that meta II is in a pH-, temperature-, and detergent-dependent equilibrium with its preceding intermediate, metarhodopsin I (meta I; Matthews et al., 1963). At pH 6 in dodecyl β-maltoside, rhodopsin has an absorption maximum at 380 nm and activates transducin, indicating that it is in its meta II state. At pH 7.5 in digitonin, rhodopsin has an absorption maximum at 480 nm and does not activate transducin. Under the latter conditions the meta I state is thought to be dominant (Franke et al., 1992; Lin & Sakmar, 1996). These observations allow for the study of the structural differences that accompany rhodopsin activation.

Proteolysis (Kuehn & Hargrave, 1981), peptide competition experiments (Koenig et al., 1989), and site-directed mutagenesis experiments (Franke et al., 1992) have indicated that the loops between helices III and IV and helices V and VI are the main targets of transducin. Using spin-labeling EPR studies on site-directed rhodopsin mutants, Farrens and co-workers found evidence that the activation of rhodopsin is induced by rigid body motion of helix VI in meta II (Farrens et al., 1996). The challenge is therefore to determine the structural factors that link retinal isomerization to this helix movement.

Several investigators have noted the involvement of aromatic amino acids in rhodopsin activation. Linear dichroism (LD) experiments by Chabre and Breton (1979) revealed significant differences between the LD spectra of rhodopsin and meta II that they attributed to the rotation of a Trp residue upon activation. In a very recent mutant absorption study, Lin et al. demonstrated that Trp_{265} and Trp_{126} undergo large changes in their environment upon meta II formation (Lin & Sakmar, 1996). It would thus be of interest to obtain structural data on the conformational and environmental changes of these aromatic amino acids using UV resonance Raman (UVRR) spectroscopy.

The vibrational spectra of aromatic amino acids can be used to probe their conformational states, hydrogen-bonding properties, and environment inside proteins (Asher, 1993; Harada & Takeuchi, 1986; Austin et al., 1993). To obtain UVRR spectra of rhodopsin and its photointermediates with a high S/N ratio, we developed a UV prefilter based on a Littrow prism spectrograph (Kaminaka & Mathies, 1997). To minimize UV photodestruction artifacts and reduce sample quantities, we also developed a new capillary flow

† This work was supported by NIH Grant EY-02051 and NSF Grant CHE 94-19714.

* Author to whom correspondence should be addressed.

⊗ Abstract published in *Advance ACS Abstracts,* October 1, 1997.

[1] Abbreviations: meta I, metarhodopsin I; meta II, metarhodopsin II; UVRR, ultraviolet resonance Raman; ROS, rod outer segment; PIPES, piperazine-*N*,*N*′-bis(2-ethanesulfonic acid); DDM, *n*-dodecyl β-D-maltoside; CCD, charge-coupled device; PSB, protonated Schiff base; EPR, electron paramagnetic resonance; LD, linear dichroism.

S0006-2960(97)01541-9 CCC: $14.00

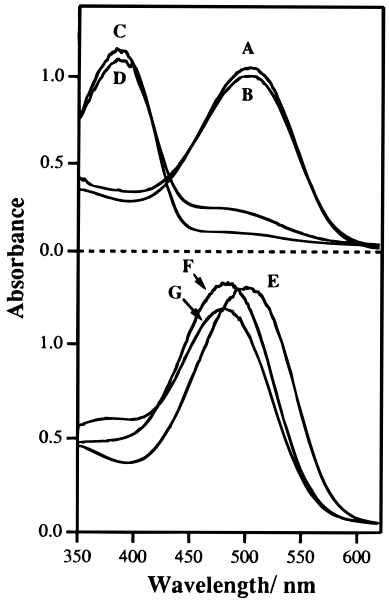

FIGURE 1: Top panel: Absorption spectra of rhodopsin in *n*-dodecyl β-D-maltoside before (A) and after (B) the UVRR experiment and absorption spectra of the meta II sample before (C) and after (D) the UVRR experiment. Bottom panel: Absorption spectrum of rhodopsin in digitonin (E) and absorption spectra of the meta I sample before (F) and after (G) the UVRR experiments.

technique. With these methods, high-quality UVRR spectra of rhodopsin can be obtained. We find that at least one tryptophan residue that resides in a highly hydrophobic, weakly hydrogen-bonding environment in rhodopsin is transferred into a less hydrophobic, non-hydrogen-bonding environment when meta I converts to meta II. These results suggest a model for rhodopsin activation in which retinal isomerization causes a disruption of the interaction of Trp_{265} with the ionone ring of retinal.

MATERIALS AND METHODS

Sample Preparation. Rod outer segments (ROS) were isolated from 100 bovine retinas (J. A. Lawson, Lincoln, NE) by sucrose flotation followed by sucrose density gradient centrifugation as described previously (Palings et al., 1987). The ROS were lysed in water and solubilized in 1% *n*-dodecyl β-D-maltoside. The rhodopsin solution was then loaded on a concanavalin A/Sepharose column that was equilibrated with buffer A [20 mM PIPES, pH 6.5, 4 mM dodecyl β-maltoside (DDM), 150 mM NaCl, 1 mM $CaCl_2$, 1 mM $MgCl_2$, 1 mM $MnCl_2$, and 0.1 mM EDTA]. The column was washed with at least 15 bed volumes of buffer A or buffer B (buffer A in which DDM was replaced by ~0.2% digitonin, pH 7.7), respectively. Rhodopsin was eluted by supplementing buffer A or buffer B with 200 mM methyl α-D-mannoside. Finally, the eluted rhodopsin was dialyzed against buffer A or buffer B to remove mannoside from the solutions. Final solutions were 20−25 μM in rhodopsin. Meta II (meta I) was prepared by illuminating rhodopsin solutions in buffer A (buffer B) placed into an ice bath with light from a 60 W light bulb filtered through a 515 nm long-pass filter for 2−3 min. This procedure yielded virtually complete conversion (>95%) of rhodopsin to its respective photoproducts. Raman spectra were taken immediately after sample photoconversion. The total spectral acquisition time for one sample was less than 1 h. Figure 1 presents the absorption spectra of the various rhodopsin, meta II, and meta I samples before and after the Raman experiments.

Raman Spectroscopy. Excitation light at 233.9 nm was generated by Raman-shifting the 532 nm output of an amplified Nd-YAG laser (DCR-2A) via the eighth anti-Stokes line of D_2. Rotational lines of D_2 were almost completely rejected using a combination of a grating with a spatial filter. Light at 233.9 nm (~25 μW) was focused (150 μm × 1 mm) onto the rhodopsin solution flowing through a 75 μm i.d. fused silica capillary at a flow rate of ~10 cm/s. The solution was pumped by immersing the capillary into a pressurized (100 psi), ice-cooled rhodopsin solution. The flow-rate ensured complete removal of the sample from the focused beam area between laser pulses. The capillary containing the sample was cooled by a stream of N_2 gas to ~2 °C. After passing through the focused beam, the sample was transferred to an ice-cooled reservoir. The reduction in the visible absorption of rhodopsin in the final reservoir after the experiment (Figure 1B) showed that ~5% of the rhodopsin was photoconverted to meta II during the experiment. Since the bleaching quantum yield is ~30% at 233 nm (Kropf, 1982), this suggests that only ~15−20% of the molecules absorbed a UV photon during the single pass through the beam. The absorption spectra of meta II (Figure 1D) and meta I (Figure 1G) after the experiment provide an upper estimate of the extent of thermal decay of the probed meta samples during the spectral acquisition. On the basis of these data, the meta I samples contained less than 10% meta II (Figure 1G), and the meta II sample contained less than 10% metarhodopsin III and/or other decay products (Figure 1D). This demonstrates that rhodopsin (>95%), meta I (>90%), and meta II (>90%) were the dominant contributors to their respective UVRR spectra.

The excitation geometry was similar to that employed in previously reported experiments (Kaminaka et al., 1990), with the exception that the angle of incidence was 135° rather than 120°. Scattered light was detected with a back-thinned, UV-sensitive CCD detector (Princeton Instruments, Model 1100 BP) coupled to a single spectrograph (Spex 500M). Rayleigh scattering was rejected with a UV prefilter based on a Littrow prism design (Kaminaka & Mathies, 1997). Wavelengths were calibrated using the Raman lines of ethanol. The spectral resolution was ~15 cm^{-1} and frequencies are accurate to ~3 cm^{-1}. The detection window extended from 500 to 4000 cm^{-1}. This allows for convenient generation of difference spectra using the water stretching bands around 3300 cm^{-1} as internal standards. The spectra were intensity-corrected using a D_2 standard lamp (Hamamatsu, LH403).

Computational Methods. A structural model of rhodopsin was built using Insight, and the protein structure was minimized using Discover (Molecular Simulations, San Diego, CA). The computational methods were described previously (Kochendoerfer et al., 1997). For initial minimization, additional torsional constraints of 25 kcal/deg were imposed on the geometry of Trp_{265} ($\chi_1 = +180$ and $\chi_2 = +75$) as deduced from the preliminary analysis of our UVRR data (Kochendoerfer, 1997) and published LD data (Chabre & Breton, 1979). These constraints were released for the final minimization.

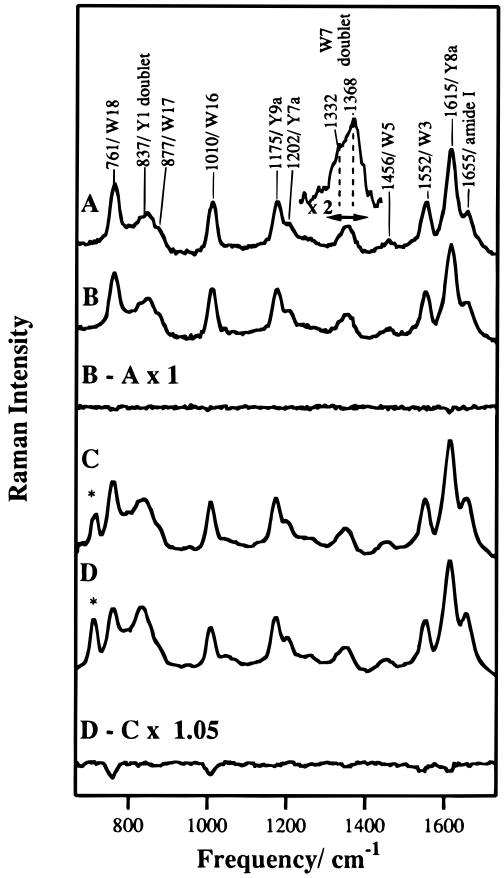

FIGURE 2: UV resonance Raman spectra of bovine rhodopsin in digitonin (A), its meta I bleaching intermediate (B), and their difference spectrum (B − A) and of bovine rhodopsin in *n*-dodecyl β-D-maltoside (C), its meta II bleaching intermediate (D), and their difference spectrum (D − C × 1.05). Spectra were excited with ~25 μW of 233.9 nm light from a DCR-2A YAG laser at 20 Hz. Lines marked with an asterisk are rotational lines from the excitation beam. The inset shows a higher resolution scan of the W7 doublet of rhodopsin in ammonyx buffer.

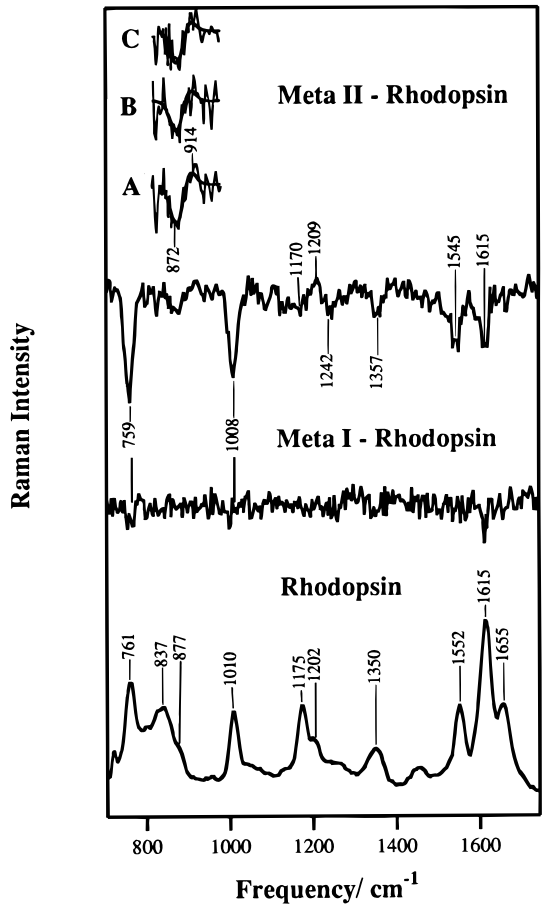

FIGURE 3: UV resonance Raman difference spectra of metarhodopsin II minus rhodopsin (top) and metarhodopsin I minus rhodopsin (middle). For comparison, a scaled (divided by 5) rhodopsin spectrum is also displayed (bottom). The insets show a fit of the meta II derivative band around 890 cm^{-1} for the combined data (A) and for the two independent raw data sets (B and C), respectively.

RESULTS

Figure 2 presents the 233.9 nm UVRR spectra of rhodopsin in digitonin and meta I and their difference spectrum, as well as those of rhodopsin in *n*-dodecyl β-D-maltoside and meta II and their difference spectrum. The spectra show contributions from the 19 tyrosine and 5 tryptophan residues of rhodopsin (Hargrave et al., 1983; Ovchinnikov et al., 1982). The protein bands are labeled according to the convention adopted by Harada and co-workers (Harada & Takeuchi, 1986). Tryptophan bands are observed at 761 (W18), 1010 (W16), ~1350 [W7 and several HOOP (hydrogen-out-of-plane) combinations], 1456 (W5), and 1552 cm^{-1} (W3) and shoulders at ~877 (W17) and ~1525 cm^{-1} (2 × W18). The W7 doublet could only be resolved with a different spectrometer configuration (see inset). Tyrosine bands are observed at ~837 (Y1 and 2 × Y16a), 1175 (Y9a), 1202 (Y7a), and 1615 cm^{-1} (Y8a). The latter band is expected to have a small contribution from the W1 mode of tryptophan. However, in mellitin, a protein devoid of tyrosine residues, the intensity of this band with 230 nm excitation is only one-third of the intensity of the 1552 cm^{-1} band (Efremov et al., 1992). This suggests that in rhodopsin this mode contributes less than 20% of the 1615 cm^{-1} band intensity. The band at 1655 cm^{-1} is due to vibrations of unsaturated hydrocarbon chains of residual membrane lipid and detergent as well as contributions from amide I vibrations.

Meta I Difference Spectra. The meta I minus rhodopsin and meta II minus rhodopsin spectra, as well as the unsubtracted rhodopsin spectrum, are presented more clearly in Figure 3. The meta I minus rhodopsin spectrum exhibits a slight decrease in intensity of the Tyr Y8a band at 1615 cm^{-1} in meta I. This band is enhanced due to vibronic coupling of the Tyr L_b band to its B_b band (Fodor et al., 1989). The intensity of this band depends on the resonance of the excitation wavelength with the L_b band of a particular tyrosine residue. The intensity reduction of the Y8a band indicates that there is an absorption shift of one or several tyrosine residues during the transition from rhodopsin to meta I. The meta I difference spectrum does not reveal any further reproducible changes involving tyrosine bands. The meta I minus rhodopsin difference spectrum shows weak negative bands at 759 and 1008 cm^{-1}. These features in the meta I spectrum may be due to either very small tryptophan environmental changes and/or scattering from a small population (<10%) of meta II in the sample.

Meta II Difference Features. The meta II minus rhodopsin difference spectra presented in Figure 3 reveal significant changes involving both Trp and Tyr bands. The most dramatic change is a large intensity decrease for the totally

symmetric tryptophan modes at 759, 1008, and 1545 cm^{-1}. The intensity of these three bands decreases by ~20%, 20%, and 10%, respectively. Since these totally symmetric modes are A-term Raman-enhanced, their intensity is a function of the resonance of the Trp B_b band (Fodor et al., 1989). The intensity decrease is therefore consistent with an absorption shift of at least one Trp residue upon conversion of rhodopsin to meta II.

The difference band at 1545 cm^{-1} in meta II is at a somewhat lower frequency compared to the 1552 cm^{-1} band observed for rhodopsin. The frequency of this Trp band is known to be sensitive to the torsional χ_2 angle of the C_β−indole bond (Miura et al., 1989). The lower frequency of this feature could have two origins. Either the band is caused by an intensity reduction of a Trp residue with a W3 frequency of 1545 cm^{-1} in both rhodopsin and meta II (Model 1) or it is due to a shifted W3 band of a Trp residue that rotates around the C_β−indole bond during the transition from rhodopsin to meta II (Model 2). To distinguish between these models, Gaussian bands with a width of 20 cm^{-1} and maxima at 1525, 1552, and 1618 cm^{-1} for Trp, 1601 and 1615 cm^{-1} for Tyr, and 1655 cm^{-1} for the amide and lipid bands were fit to the rhodopsin UVRR spectrum.[2] To model the difference spectra, the intensities of the relevant Tyr and Trp bands were reduced, and the frequency of the band at ~1545 cm^{-1} was shifted by 0, 4, and 7 cm^{-1}, and the meta II bands were subtracted. We find that adding a frequency shift to produce the negative feature at 1545 cm^{-1} also results in a positive feature at ~1566 cm^{-1}, which is not observed in the experimental data. The difference band at 1545 cm^{-1} therefore suggests that one or more Trp residues do not undergo significant rotation around their C_β−indole bond but rather experience an environmental change affecting their W3 Raman intensity. The W3 difference frequency at 1545 cm^{-1} correlates with a χ_2 angle of ~±75° for the particular Trp residue in both rhodopsin and meta II.

A second significant feature in the meta II minus rhodopsin difference spectrum in Figure 3 is a negative band centered at 1357 cm^{-1}. For tryptophan in solution and in most proteins, this frequency region typically exhibits a doublet at ~1360 and 1340 cm^{-1}, which arises from the interaction of the W7 mode with several out-of-plane modes (Harada & Takeuchi, 1986). The intensity ratio I_{1360}/I_{1340} is known to be a measure of the hydrophobicity of the environment of a particular Trp residue. It varies from 0.7−0.9 in hydrophilic solvents to 1−1.1 in benzene and its derivatives and up to 1.2−1.3 in saturated hydrocarbons (Miura et al., 1988). Whereas this correlation was established exciting off-resonance, previously published results suggest that it also holds under resonant ~235 nm excitation (Jordan et al., 1995; Sweeney et al., 1991). Due to the contribution of five different Trp residues to this doublet, we were not able to resolve the doublet for rhodopsin. The I_{1368}/I_{1332} intensity ratio in the higher resolution inset in Figure 2 is ~1.3, suggesting that most of the Trp residues in rhodopsin are located in hydrophobic environments. The shape of the meta II difference spectrum, which exhibits a negative band at 1357 cm^{-1}, but no significant intensity change at ~1340 cm^{-1}, suggests that the W7 doublet in meta II exhibits both an intensity reduction and an intensity redistribution between its components compared to rhodopsin. Our result therefore suggests that the environment of one or more Trp residues becomes less hydrophobic after rhodopsin activation.

A third change in the meta II minus rhodopsin difference spectrum is the appearance of a derivative feature with a negative peak at 872 cm^{-1} and a small positive peak at 914 cm^{-1} that is attributed to a shifted W17 band. Though weak, this difference feature was reproduced in two independent data sets as presented in Figure 3. This feature was adequately modeled by subtracting the 885 cm^{-1} W17 band in rhodopsin from the meta II W17 band at ~892 cm^{-1} (see insets in Figure 3). Miura et al. (1988) studied a series of crystal structures of tryptophan salts and found a correlation between the frequency of the W17 band and the Trp hydrogen-bonding strength. The values measured here lie outside the experimental range observed for the W17 mode of Trp model compounds. Since hydrogen-bonding strength is the only known determinant of W17 frequencies, we extrapolate the correlation found by Miura and assign the W17 frequency of 885 cm^{-1} to a weakly hydrogen-bonded Trp residue and the W17 frequency of 892 cm^{-1} to a non-hydrogen-bonded Trp residue. This result suggests that one or more Trp residues experience a reduction in hydrogen-bonding strength upon meta II formation.

The most obvious tyrosine feature in the meta II minus rhodopsin difference spectrum in Figure 3 is the intensity reduction of the Y8a band at 1615 cm^{-1} in meta II. This feature is most likely superimposed on a small negative contribution of the Trp W1 band. Possible additional difference features can be discerned in the Tyr fingerprint region at 1170, 1209, and 1242 cm^{-1}. These bands may represent difference features of shifted Y7a′, Y7a, and/or Y9a bands of one or several tyrosine residues or intensity changes of the individual bands.

DISCUSSION

UV Resonance Raman Spectroscopy. UVRR experiments on rhodopsin solutions recirculating between the reservoir and sampling point showed that prolonged spectral acquisition with 230 and 235 nm excitation causes UV destruction and introduces artifacts in the rhodopsin difference spectra. To avoid these artifacts, we developed a capillary flow technique that has several advantages over the previous setup. First, the sample is passed only once across the sampling point, ensuring that the probed protein molecules have not been previously exposed to UV light. Second, only very small amounts of sample are required for long spectral acquisitions (2 mL of rhodopsin/h). Finally, pumping rhodopsin with pressurized gas avoids warming of thermally metastable rhodopsin intermediates inside a pump, while ensuring that the sample at the sampling point is completely replaced between laser pulses. This novel setup in combination with our Littrow prism UV prefilter (Kaminaka & Mathies, 1997) opens the door for the study of bovine rhodopsin and its mutants via UV resonance Raman spectroscopy.

Protein Structural Changes in Meta II. Comparison of the meta I and meta II difference spectra demonstrates the important role of aromatic amino acids in the activation of rhodopsin. In the meta I minus rhodopsin difference spectrum (both *inactive* receptor states), little change is

[2] The 1578 cm^{-1} mode of Trp was not included in the fitting since it does not carry significant Raman intensity with 233.9 nm excitation (Efremov et al., 1992; Harada & Takeuchi, 1986).

observed. However, the protein conformational change in meta II (the *active* state) involves large environmental and significant hydrogen-bonding changes of aromatic amino acid residues. The UVRR difference spectra of Trp residues in meta II provide specific information on changes in their hydrophobicity and hydrogen-bonding patterns. In particular, the intensity ratio I_{1360}/I_{1340} is a measure of the hydrophobicity of the environment of a particular Trp residue. A decrease of I_{1360}/I_{1340} is observed during protein unfolding of cytochrome *c*, a process associated with the transfer of Trp residues from a very hydrophobic site in the protein interior to less hydophobic sites (Jordan et al., 1995). A similar observation has been made for the denaturation of azurin (Sweeney et al., 1991). The presence of a negative difference band at 1357 cm^{-1}, but not at ~1340 cm^{-1} in our meta II minus rhodopsin spectra, is therefore an indication of a reduction in environmental hydrophobicity of at least one Trp residue associated uniquely with the formation of meta II.

The derivative feature at ~890 cm^{-1} is assigned to a weakly hydrogen-bonded Trp residue with a W17 frequency at 885 cm^{-1} in rhodopsin that experiences a frequency increase of 7 cm^{-1} due to reduced hydrogen bonding upon meta II formation. This assignment is supported by FTIR difference spectra of rhodopsin and its photointermediates (Kandori & Maeda, 1995; Maeda et al., 1993). Maeda and co-workers observed a difference band at 3463 cm^{-1} that they assigned to the N−H stretching mode of a Trp residue in rhodopsin. Using the results of Miura et al. (1988), this correlates with a W17 frequency of ~882 cm^{-1}, consistent with our result. The band at 3463 cm^{-1} undergoes a slight upshift by ~25 cm^{-1} during bathorhodopsin formation and does not undergo any further change in meta I. This is consistent with our data on meta I, since a 25 cm^{-1} shift of the N−H stretching mode correlates with only a 1 cm^{-1} shift of the W17 mode. Most interestingly, a new band appears in the meta II FTIR difference spectra at 3641 cm^{-1} that was assigned to a water band (Maeda et al., 1993). However, it might also contain contributions from a Trp N−H stretching band of an isolated, perhaps sterically hindered Trp residue, since its frequency correlates with a W17 frequency of ~890 cm^{-1}, which is very similar to the value observed in our UVRR difference spectra.

Comparison to Octopus Rhodopsin. Hashimoto et al. (1996) recently published 244 nm excited UVRR difference spectra of octopus rhodopsin and its signaling acid metarhodopsin state. The difference spectra of octopus rhodopsin are very similar to the difference spectra presented here for bovine rhodopsin, suggesting that both rhodopsins undergo similar conformational changes upon activation. Despite the lower S/N ratio upon excitation at 244 nm, slight intensity reductions of the Trp bands at 1549 cm^{-1} (shifted down by 4 cm^{-1} compared to the octopus rhodopsin spectrum) and 1006 cm^{-1} and of the Tyr bands at 1615, 1209, and 1174 cm^{-1} are observed. The intensity reduction of the Y8a mode at 1615 and 1170 cm^{-1} is smaller for bovine rhodopsin than for octopus rhodopsin. It is appealing to assign these changes in octopus rhodopsin to Tyr_{112}, a residue that has no homology in bovine rhodopsin and serves as the Schiff base counterion (Ovchinnikov et al., 1988). The similarity of the Trp difference spectra between octopus and bovine rhodopsin is consistent with their sequence homology (Ovchinnikov et al., 1982, 1988), the similarity of their low-

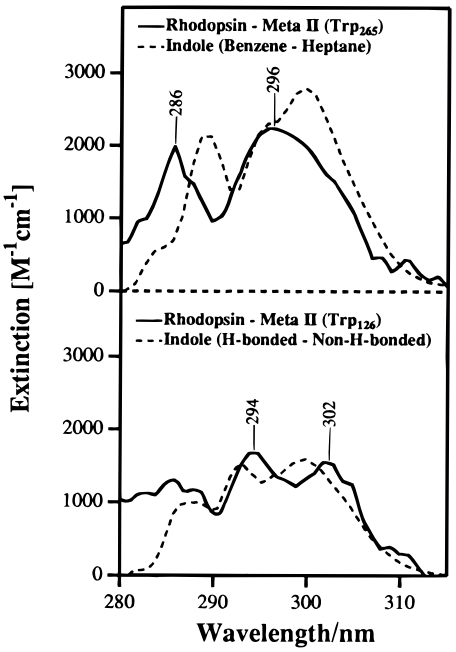

FIGURE 4: Top panel: Comparison of the rhodopsin minus meta II absorption difference spectrum for Trp_{265} (solid line) with the difference spectrum of 2,3-dimethylindole (dashed line) in benzene (n = 1.50) minus that in 2-methylheptane (n = 1.39). Bottom panel: Comparison of the rhodopsin minus metarhodopsin II absorption difference spectrum for Trp_{126} (solid line) with the difference spectrum of 2,3-dimethylindole in methylcyclohexane in the presence and absence of the strong hydrogen bond acceptor *N,N*-dimethylacetamide (dashed line). The maximum extinctions in the 2,3-dimethylindole spectra were normalized to 8000 M^{-1} cm^{-1}, a value typically observed for Trp inside a protein, prior to subtraction. The experimental mutant difference spectra are adapted from Lin & Sakmar (1996).

resolution electron-diffraction structure (Davies et al., 1996; Unger & Schertler, 1995) and the fact that both receptors transmit their signal to a transducin GTPase (Hofmann et al., 1995; Terakita et al., 1993). This suggests that activation-related protein structural changes in the vicinity of the hydrophobic ionone ring are similar in vertebrate and invertebrate species.

Possible Assignment of the UVRR Difference Features to Trp_{265}. Using a combination of site-directed mutagenesis and UV absorption spectroscopy, Lin and Sakmar recently determined that Trp_{265} and Trp_{126} are the only rhodopsin tryptophan residues whose L_a absorption band changes upon conversion to meta II. Their double-difference spectra of the absorption changes of Trp_{265} and Trp_{126} during the rhodopsin to meta II transition are reproduced in Figure 4. The rhodopsin minus meta II absorption difference spectra of Trp_{265} exhibit a broad positive band at 296 nm and a narrow satellite band at 286 nm, and the spectra of Trp_{126} exhibit two discernible peaks at 294 and 302 nm. These difference bands were assigned to the L_a absorption bands of these two residues that both undergo a blue shift upon formation of meta II (Lin & Sakmar, 1996). Bailey and co-workers observed that the L_a and B_b absorption bands undergo parallel solvent-induced shifts in tryptophan analog compounds (Bailey et al., 1968). These results limit the possible assignment of our UVRR difference bands to Trp_{265} and/or Trp_{126}, since only residues undergoing significant B_b absorption shifts can produce the large observed UVRR intensity changes.

A comparison of the mutant absorption difference spectra with the difference spectra of model compounds in different solvent systems was performed to correlate the experimental tryptophan absorption changes with environmental changes. The line width and position of the absorption band of Trp are a function of its environment (Pierce & Boxer, 1996; Strickland et al., 1972). Since the fine structure of an absorption difference spectrum is determined by the shape of the subtracted spectra (Demchenko, 1986), the absorption difference spectra contain information on the environmental change of the particular Trp residues. The shape of the rhodopsin minus meta II absorption difference spectrum for Trp_{265} is similar to the absorption difference spectrum between 2,3-dimethylindole in the very polarizable solvent benzene ($n = 1.50$) and the less polarizable solvent 2-methylheptane ($n = 1.39$) (Figure 4, top, dashed line). This suggests that the absorption shift for Trp_{265} is due to a transfer of this residue from a highly polarizable to a less polarizable environment. Trp_{265} is located adjacent to the highly polarizable retinal chromophore of rhodopsin (Nakanishi et al., 1995), consistent with this interpretation. The shape of the rhodopsin minus meta II absorption difference spectrum for Trp_{126} is similar to the absorption difference spectrum of 2,3-dimethylindole in the presence and absence of the strong hydrogen bond acceptor *N*,*N*-dimethylacetamide (Figure 4, bottom, dashed line). This suggests that the Trp_{126} absorption change originates from the transfer of this residue from a strongly hydrogen-bonding environment in rhodopsin to a weakly hydrogen-bonding environment in meta II. Since the most important contributor to the rhodopsin minus meta II UVRR difference spectrum is a tryptophan residue that transfers from a highly hydrophobic (polarizable) environment to a less hydrophobic environment during rhodopsin activation and since this residue is weakly hydrogen-bonded in the rhodopsin state, we speculate that Trp_{265}, and not Trp_{126}, is the main contributor to the observed UVRR difference spectra. The lesser contribution of Trp_{126} to the UVRR difference spectra suggests that its absorption bands in rhodopsin are less red-shifted and/or undergo a smaller shift after rhodopsin activation (Kochendoerfer, 1997). The latter explanation is consistent with its smaller difference extinction coefficient in the absorption difference spectra.

Our attribution of the UVRR difference spectra to Trp_{265} is supported by two additional observations. First, octopus rhodopsin exhibits similar tryptophan UVRR difference features between the inactive and the signaling form. This difference cannot be due to Trp_{126}, since octopus rhodopsin has a methionine in the position homologous to Trp_{126} in bovine rhodopsin. Finally, FTIR difference spectroscopy revealed that the N−H stretching band of the Trp residue, whose frequency correlates with the residue undergoing changes in the meta II UVRR difference spectra, experiences a slight frequency shift after formation of bathorhodopsin (Kandori & Maeda, 1995). Protein changes that early in the bleaching sequence are expected to occur in the vicinity of the retinal chromophore. While our rhodopsin model and chemical cross-linking studies (Nakanishi et al., 1995) put Trp_{265} next to the retinal chromophore, Trp_{126} is more than 10 Å away. This is consistent with the idea that most of the Trp changes observed in the meta II UVRR difference spectra are due to protein structural changes that are connected with environmental changes of Trp_{265}. Future UVRR experiments on site-directed rhodopsin mutants will be useful in testing this suggestion.

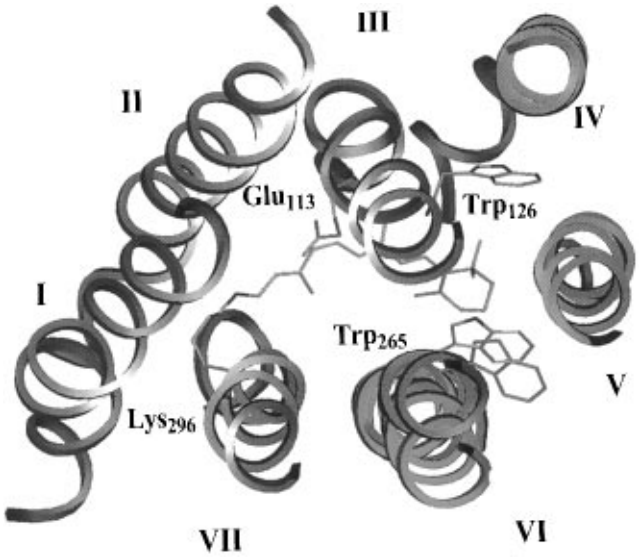

FIGURE 5: Structural model illustrating the latch-key mechanism of rhodopsin activation. The rhodopsin helices are shown in gray, and rhodopsin residues and the retinal chromophore are shown in CPK colors. Light-induced isomerization disrupts the interaction of Trp_{265} with retinal, resulting in displacement of helix VI without a change in Trp_{265} conformation (Farrens et al., 1996). The proposed new position of Trp_{265} and the resulting tilt and rotation of helix VI are shown in red. Rigid body movement of helix VI results in loop conformational changes followed by signal amplification.

CONCLUSION

Figure 5 presents a structural model illustrating a possible "latch-key" mechanism for rhodopsin activation. In rhodopsin, Trp_{265} strongly interacts with the retinal chromophore and is locked under the ionone ring. Light-induced isomerization of the chromophore might move its ionone ring away from helix VI, closer to helix III (Nakanishi et al., 1995). This movement disrupts the interaction of Trp_{265} with the ionone ring. As shown in red, this disruption might allow Trp_{265} to slip past the ionone ring and helix VI to tilt away from the membrane plane (Farrens et al., 1996). The importance of the Trp_{265}−ionone interaction in the activation of G-protein-coupled receptors is supported by the presence of this residue in more than 96% of all sequenced receptors (Baldwin, 1993). Both mutation of Trp_{265} (Nakayama & Khorana, 1991) and removal of the ionone ring in analog rhodopsins (Jaeger et al., 1994) severely impede the activation of rhodopsin. The rigid-body movement of helix VI then alters the conformation of the cytoplasmic loops, which is detected by transducin. It will now be interesting to perform UVRR experiments on other G-protein coupled receptors in the presence and absence of agonist to establish the generality of this activation mechanism.

ACKNOWLEDGMENT

We thank Steve W. Lin for many helpful discussions, Cuong Vuong for expert assistance with the rhodopsin preparations, and Jim Scherer and Michael J. Tauber for valuable technical discussions during the development of the capillary flow system. We also thank Steve W. Lin and Tom P. Sakmar for providing the rhodopsin mutant absorption difference spectra.

REFERENCES

Asher, S. A. (1993) *Anal. Chem. 65*, 201A−210A.

Austin, J. C., Rodgers, K. R., & Spiro, T. G. (1993) *Methods Enzymol. 226*, 374−396.

Bailey, J. E., Beaven, G. H., Chignell, D. A., & Gratzer, W. B. (1968) *Eur. J. Biochem. 7*, 5−14.

Baldwin, J. M. (1993) *EMBO J. 12*, 1693−1703.

Chabre, M., & Breton, J. (1979) *Photochem. Photobiol. 30*, 295−299.

Davies, A., Schertler, G. F. X., Gowen, B. E., & Saibil, H. R. (1996) *J. Struct. Biol. 117*, 36−44.

Demchenko, A. P. (1986) *Ultraviolet Spectroscopy of Proteins*, Springer-Verlag, Berlin and New York.

Efremov, R. G., Feofanov, A. V., & Nabiev, I. R. (1992) *J. Raman Spectrosc. 23*, 69−73.

Farrens, D. L., Altenbach, C., Yang, K., Hubbell, W. L., & Khorana, H. G. (1996) *Science 274*, 768−770.

Fodor, S. P. A., Copeland, R. A., Grygon, C. A., & Spiro, T. G. (1989) *J. Am. Chem. Soc. 111*, 5509−5518.

Franke, R. R., Sakmar, T. P., Graham, R. M., & Khorana, H. G. (1992) *J. Biol. Chem. 267*, 14767−14774.

Harada, I., & Takeuchi, H. (1986) *Advances in Spectroscopy: Spectroscopy of Biological Systems* (Clark, R. J. H., & Hester, R. E., Eds.) pp 113−175, Wiley, New York.

Hargrave, P. A., McDowell, J. H., Curtis, D. R., Wang, J. K., Juszczak, E., Fong, S.-L., Rao, J. K. M., & Argos, P. (1983) *Biophys. Struct. Mech. 9*, 235−244.

Hashimoto, S., Takeuchi, H., Nakagawa, M., & Tsuda, M. (1996) *FEBS Lett. 398*, 239−242.

Hofmann, K. P., Jaeger, S., & Ernst, O. P. (1995) *Isr. J. Chem. 35*, 339−355.

Jaeger, F., Jaeger, S., Kraeutle, O., Friedman, N., Sheves, M., Hofmann, K. P., & Siebert, F. (1994) *Biochemistry 33*, 7389−7397.

Jordan, T., Eads, J. C., & Spiro, T. G. (1995) *Protein Sci. 4*, 716−728.

Kaminaka, S., & Mathies, R. A. (1997) *Appl. Spectrosc.*, in press.

Kaminaka, S., Ogura, T., & Kitagawa, T. (1990) *J. Am. Chem. Soc. 112*, 23−27.

Kandori, H., & Maeda, A. (1995) *Biochemistry 34*, 14220−14229.

Kliger, D. S., & Lewis, J. W. (1995) *Isr. J. Chem. 35*, 289−307.

Kochendoerfer, G. G. (1997) Ph.D. Thesis, University of California at Berkeley.

Kochendoerfer, G. G., & Mathies, R. A. (1995) *Isr. J. Chem. 35*, 211−226.

Kochendoerfer, G. G., Wang, Z., Oprian, D. D., & Mathies, R. A. (1997) *Biochemistry 36*, 6577−6587.

Koenig, B., Arendt, A., McDowell, J. H., Kahlert, M., Hargrave, P. A., & Hofmann, K. P. (1989) *Proc. Natl. Acad. Sci. U.S.A. 86*, 6878−6882.

Kropf, A. (1982) *Methods Enzymol. 81*, 384−392.

Kuehn, H., & Hargrave, P. (1981) *Biochemistry 20*, 2410−2417.

Lin, S. W., & Sakmar, T. P. (1996) *Biochemistry 35*, 11149−11159.

Maeda, A., Ohkita, Y. J., Sasaki, J., Shichida, Y., & Yoshizawa, T. (1993) *Biochemistry 32*, 12033−12038.

Matthews, R. G., Hubbard, R., Brown, P. K., & Wald, G. (1963) *J. Gen. Physiol. 47*, 215−240.

Miura, T., Takeuchi, H., & Harada, I. (1988) *Biochemistry 27*, 88−94.

Miura, T., Takeuchi, H., & Harada, I. (1989) *J. Raman Spectrosc. 20*, 667−671.

Nakanishi, K., Zhang, H., Lerro, K. A., Takekuma, S., Yamamoto, T., Lien, T. H., Sastry, L., Baek, D., Moquin-Pattey, C., Boehm, M. F., Derguini, F., & Gawinowicz, M. A. (1995) *Biophys. Chem. 56*, 13−22.

Nakayama, T. A., & Khorana, H. G. (1991) *J. Biol. Chem. 266*, 4269−4275.

Ovchinnikov, Y. A., Abdulaev, N. G., Feigina, M. Y., Artamonov, I. D., Zolotarev, A. S., Kostina, M. B., Bogachuk, A. S., Miroshnikov, A. I., Martinov, V. I., & Kudelin, A. B. (1982) *Bioorg. Khim. 8*, 1011−1014.

Ovchinnikov, Y. A., Abdulaev, N. G., Zolotarev, A. S., Artamonov, I. D., Bespalov, I. A., Dergachev, A. E., & Tsuda, M. (1988) *FEBS Lett. 232*, 69−72.

Palings, I., Pardoen, J. A., van den Berg, E., Winkel, C., Lugtenburg, J., & Mathies, R. A. (1987) *Biochemistry 26*, 2544−2556.

Pierce, D. W., & Boxer, S. G. (1995) *Biophys. J. 68*, 1583−1591.

Schoenlein, R. W., Peteanu, L. A., Mathies, R. A., & Shank, C. V. (1991) *Science 254*, 412−415.

Strickland, E. H., Billups, C., & Kay, E. (1972) *Biochemistry 11*, 3657−3662.

Sweeney, J. A., Harmon, P. A., Asher, S. A., Hutnik, C. M., & Szabo, A. G. (1991) *J. Am. Chem. Soc. 113*, 7531−7537.

Terakita, A., Hariyama, T., Tsukahara, Y., Katsukura, Y., & Tashiro, H. (1993) *FEBS Lett. 330*, 197−200.

Unger, V., & Schertler, G. F. X. (1995) *Biophys. J. 68*, 1776−1786.

BI971541C